We have performed computer simulation calculations with a broadband pump using the one-dimensional–particle simulation code we have used in the past.[13] We find the same results as in the measurements. Well above threshold, where significant suprathermal electrons are produced, the growth rate decreases with increasing bandwidth, but the instability saturation level and suprathermal-electron production are not a strong function of bandwidth.

In summary, we have observed that the ensemble-averaged high-frequency–wave energy grows exponentially as if the waves were excited by a coherent pump wave for small enough pump bandwidth. The growth rate decreases with increasing bandwidth as if only the fraction of the pump power within the resonance width is available to drive the waves, in agreement with theoretical predictions. The saturation level and suprathermal-electron production well above threshold are almost independent of bandwidth. The waves still grow for large bandwidth, but not exponentially. This nonexponential growth will be investigated further.

We are indebted to J. J. Thomson, C. P. DeNeef, and A. J. Theiss for useful discussions. The expert assistance of T. Faulkner and T. Hillyer is gratefully acknowledge. One of us (K. M.) acknowledges support for this work by Lawrence Livermore Laboratory under Intramural Orders 9037305 and 3233503; another (J. S. DeG.) acknowledges support by the U. S. Air Force Office of Scientific Research under Grant No. 72-2290.

[1]T. K. Chu and H. W. Hendel, Phys. Rev. Lett. 29, 634 (1972); J. J. Thomson, R. J. Faehl, W. L. Kruer, and S. Bodner, Phys. Fluids 17, 973 (1974).

[2]H. Dreicer, R. F. Ellis, and J. C. Ingraham, Phys. Rev. Lett. 31, 426 (1973).

[3]K. Mizuno and J. S. DeGroot, Phys. Rev. Lett. 35, 219 (1975), and University of California, Davis, Report No. UCD PRG-R25 (to be published).

[4]J. H. Nuckolls, in *Laser Interaction and Related Plasma Phenomena* (Plenum, New York, 1974), Vol. 3B.

[5]G. M. Zaslavskii and V. E. Zakharov, Zh. Tekh. Fiz. 37, 10 (1967) [Sov. Phys. Tech. Phys. 12, 7 (1967)]; S. Tamor, Phys. Fluids 16, 1169 (1973); G. Laval, R. Pellat, and D. Pesme, Phys. Rev. Lett. 36, 192 (1976).

[6]E. J. Valeo and C. R. Oberman, Phys. Rev. Lett. 30, 1035 (1973).

[7]J. J. Thomson, Nucl. Fusion 15, 237 (1975).

[8]C. Yamanaka, T. Yamanaka, T. Sasaki, J. Mizui, and H. B. Kang, Phys. Rev. Lett. 32, 1038 (1974).

[9]S. P. Obenschain, N. C. Luhmann, Jr., and P. T. Greiling, Phys. Rev. Lett. 36, 1309 (1976).

[10]K. Mizuno and J. S. DeGroot, University of California, Davis, Report No. UCD PRG-R-16 (to be published).

[11]In order to apply the infinite-plasma theory, we have noted that the parametrically excited waves do not convect out of the mesh waveguide.

[12]This intuitive formula gives results in fairly good agreement with the results from Eq. (1).

[13]J. S. DeGroot and J. E. Tull, Phys. Fluids 18, 672 (1975).

Enhanced Backscatter with a Structured Laser Pulse

B. H. Ripin, F. C. Young, J. A. Stamper, C. M. Armstrong, R. Decoste, E. A. McLean, and S. E. Bodner

Naval Research Laboratory, Washington, D. C. 20375

(Received 13 July 1977)

A large-amplitude backscatter instability, consistent with Brillouin, occurs when a prepulse plasma is formed ahead of a high-irradiance (10^{15}–10^{16} W/cm^2) Nd-laser pulse. These results indicate that temporally structured laser pulses suggested for laser pellet implosion may also encounter large backscatter.

Precise laser-pulse temporal shaping and good laser-light absorption are usually required for successful implosion of laser-fusion pellets.[1] In the experiments reported here we simulate the effect of a shaped pulse by first forming a plasma blowoff with a prepulse and then irradiating this preformed plasma with a short, high-irradiance main pulse. The low-density plasma resulting from the prepulse is likely to be similar to that produced by the long leading portion of some currently planned, shaped pulses. Measurements show greatly enhanced direct backscatter[2] (by up to a factor of 3) and significantly reduced absorption of the second (main) pulse (in some cases to about 20%) in the presence of a prepulse-formed plasma. This backscatter appears to originate in the underdense region of the plasma ($n \lesssim 0.1 n_c$) and exhibits many of the properties of the Bril-

louin backscatter instability.[3,4] No saturation of the backscatter instability appears in the energy range of this experiment. These results suggest that many of the shaped pulses proposed for laser fusion may have very poor coupling to the target plasma. The behavior of scattered light, x-rays, high-energy ions and electrons, harmonic emission, and density profile were obtained as functions of the prepulse level, the angle of irradiation of a planar target, and the incident laser intensity.

One beam of the Naval Research Laboratory Pharos II Nd laser operating at 1.06 μm, 75-psec pulse duration (full width at half-maximum) was focused with a $f/1.9$ aspheric lens onto the surface of polished planar polystyrene (CH) targets in an evacuated chamber. A controlled prepulse was introduced into the beam with the beam splitting arrangement shown in Fig. 1(a). The relative timing of the prepulse to the main pulse was set at 2 nsec and the relative amplitudes were varied with attenuators A_p and A_m. Any unintentional prepulses were suppressed to below 10^{-7} of the total pulse energy by two saturable absorber cells and one Pockels cell in the laser chain. Three prepulse monitors were used on each shot to measure values of the ratio of the prepulse to the main pulse ranging from 10^{-8} to 1. The half-energy-content focal diameter was determined to be 30 μm by the multiple-image thin-film ablation method[5] yielding average and peak irradiances (for 9 J incident) of 7.5×10^{15} and $I\times10^{17}$ W/cm^2, respectively, at normal incidence. A focal-shift monitor was used to ensure on most shots that the target was in focus.[6]

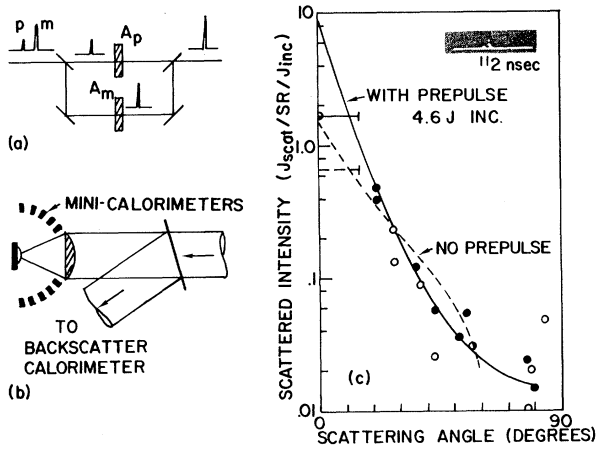

FIG. 1. (a) Diagram of the optical path of the laser beams in the prepulse generator. (b) Diagram of the scattered-light calorimeter layout. (c) Angular distributions of all scattered light for a typical single-pulse shot (dashed line) and a shot with a prepulse (solid line); (●) $\perp$ plane, (○) $\parallel$ plane. Horizontal bars between 0 and 15° are the backward reflections averaged over the lens solid angle. Backward reflection and total absorption are (15%, 50%) for the single pulse and (45%, 20%) for the double pulse, respectively.

Diagnostics operating on these experiments included incident and backward reflection calorimeters, and an array of eighteen minicalorimeters, all calibrated to ±5% accuracy [see Fig. 1(b)]. On each shot the calorimeter array measured the angular distributions of scattered laser light both within ($\parallel$) and normal to ($\perp$) the plane containing the electric vector and wave vector of the incident laser beam. Also, fifteen filtered detectors for continuum x rays from 1 to 600 keV, a magnetic electron spectrometer (50–500 keV), an ion-charge collector (10–150 keV H^+), and a silicon photodiode and spectrograph for monitoring laser harmonic emission ($n\lesssim5$) were employed. Interferometry of the prepulse-formed plasma at the arrival time of the second pulse was accomplished with use of a Raman-shifted second-harmonic probe beam ($\lambda=6329$ Å, time duration $\cong35$ psec) to obtain underdense plasma scale lengths and to ensure that single-pulse cases had no prepulse plasma. The electron, ion, and x-ray detectors, the harmonic emission, and the interferometer were all viewing the plasma approximately midway between the $\parallel$ and $\perp$ planes of polarization of the incident laser beam. All detectors were near 45° to the target normal except for the four most energetic x-ray detectors and the interferometer which viewed the plasma tangent to the target surface at normal incidence.

An example of the effect of a prepulse upon the scattered-light angular distribution, and therefore absorption efficiency, is shown in Fig. 1(c). When a prepulse plasma is present, a dramatic increase of backward reflection is seen compared to that measured without initial plasma at the target surface. The absorption decreases from about 50% without prepulse to 20% with the prepulse. The change in the angular distribution at angles outside the solid angle of the lens is not dramatically affected except possibly near 90° (which does not represent a large fraction of the scattered energy).

The dependence of the backscattered energy of the main pulse upon the prepulse/total-energy ratio, η, is shown in Fig. 2(a) for incident energies in the range of 7 to 11 J. For $\eta\gtrsim10^{-4}$, a significant and monotonically increasing backscatter (to over 40%) is observed over that for a sin-

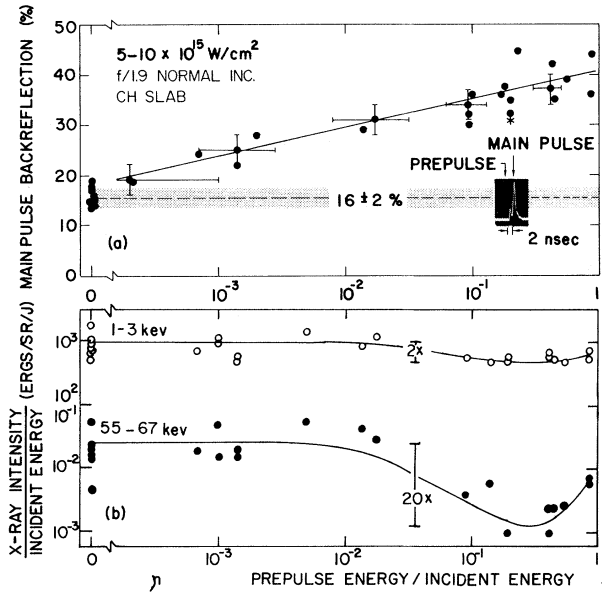

FIG. 2. (a) Backward reflections of the main pulse versus prepulse level showing enhanced backscatter for $\eta \gtrsim 10^{-4}$. Hashed region is the single-pulse backreflection. (b) X-ray intensities for 1–3-keV and 55–67-keV x rays versus prepulse level illustrating the decrease in intensity and spectral hardness of x rays with increasing η. (Increase in intensity for η approaching unity is due to x-ray emission induced by the prepulse itself.)

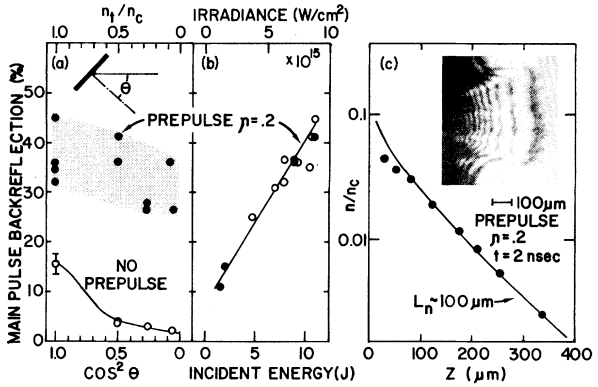

FIG. 3. Backward reflections of the main laser pulse versus (a) target angle θ (or turning-point density), and (b) the incident energy or irradiance [(○) $\theta = 0°$, (●) $\theta = 45°$]. (c) Interferogram and Abel-inverted axial electron density profile of the prepulse plasma at the time of arrival of the main pulse.

gle-pulse irradiation.[7] These data exhibited excellent reproducibility when η was varied at random from shot to shot over the course of many days. Shots were taken with the prepulse alone (second pulse blocked) to ensure that the backward reflection for a prepulse was the same as for a single pulse (they were) and to measure the prepulse energy directly as a check on the prepulse diode monitors. Included in Fig. 2(a) is a shot for $\eta = 0.2$ where the laser was focused upon the prepulse plasma rather than on the target surface. Enhanced backscatter was observed under this condition as well.[8]

All other plasma emissions (x rays, energetic ions and electrons, and harmonic emission) decreased with increasing prepulse level for $\eta > 10^{-3}$. Responses of two of the x-ray detectors (normalized to incident energy) are plotted as a function of prepulse level in Fig. 2(b). A decrease in both x-ray intensity and hardness of the x-ray spectrum with increasing prepulse level is indicated. An obvious explanation for the decreased plasma emission with increasing prepulse level is the lowered irradiance and absorption in the critical and one-fourth critical regions of the plasma.

The enchanced backscatter occurring when the laser pulse irradiates a preformed plasma strongly suggests the action of a backscatter instability mechanism being operative.[3,4] Measurements were made with the target rotated through various angles θ from normal incidence to test for the following two properties of Brillouin backscatter: First, a backscatter instability should cause the light to return through the focusing lens, regardless of the target angle. Second, the incident laser light penetrates the plasma up to the turning-point density n_t, below the critical density n_c, given in plane geometry by $n_t = n_c \cos^2\theta$. Thus, the target angle at which the enhanced backscatter effect drops off is indicative of the plasma density where the backscattering instability occurs. The results of backscatter measurements with and without a prepulse as a function of target angle are shown in Fig. 3(a). With no prepulse the backward reflection quickly drops off with angle as reported previously.[9] However, with an $\eta = 0.2$ prepulse plasma the *direct* backscatter remains high even for target angles $> 75°$, i.e., within 15° of grazing incidence! Here the stimulated backscatter is more than an *order of magnitude* larger than that for a single pulse. For $\theta = 82°$ it was verified that the reflected rays retrace the incident rays by first blocking half of the focusing lens and then looking (unsuccessfully) for backscatter in the blocked half with burnpaper. Therefore, the density of the backscattering region is below $0.1 n_c$, assuming that the low-density plasma is approximately one dimensional.[10]

All of these properties—enhanced backscatter regardless of target angle, ray retracing, and backscatter occurring in the underdense region—are consistent with stimulated Brillouin backscatter. The nature of these properties of the large directed backscatter suggests that variations of target geometry (e.g., spherical) are not likely to alter this basic effect.

Figure 3(b) shows the incident energy dependence of the backscatter with an $\eta = 0.2$ prepulse Enhanced backscatter is still present even though the beam energy is reduced by a factor of 10, i.e., to about 5×10^{14} W/cm^2 for the second pulse, and there is no indication of saturation of the instability with increasing energy.

Interferograms of the prepulse-formed plasma at the time of arrival of the main pulse, such as that shown in Fig. 3(a), indicate the presence of long scale lengths in density (~ 100 μm) below $0.1n_c$ which are ideal for good growth of the Brillouin instability. The threshold for the Brillouin instability is well below all irradiances used here for the second pulse.

Brillouin backscatter convectively saturates with a net gain of exp(λ), with $\lambda = 2\pi\gamma_0^2/(cc_s dK/dx)$, where γ_0 is the homogeneous-growth rate, c_s is the ion acoustic velocity, and $K(x)$ is the wave-number mismatch of the pump and scattered waves.[3] Mismatch is usually ascribed to plasma density and velocity gradients. There is, however, another mismatch that is present even for a uniform plasma: the spatial gradients of the laser wave near the focus of a lens. This correlation length is usually referred to as the depth of focus. For example, a plane wave incident on a simple lens has on-axis distances between nulls of $\pm 8F^2\lambda_0$, where F is the f number of the lens. For a laser or lens with aberrations, the correlation length (not the null distance) could be even less. (Away from focus, the correlation length will increase.) There are thus two basic scale lengths: the light-correlation length and the plasma-density gradient. The role of the laser prepulse may be to increase the underdense plasma-density scale length, and to increase the number of correlation lengths for the scatter, while the light correlation length controls the mismatch. This may explain the relatively weak dependence of the scatter on prepulse energy. We do not yet have sufficient data to determine accurately the gain, exp(λ).

These experiments, which use a prepulse to simulate a temporally shaped pulse, strongly suggest that significant Brillouin backscatter may also occur in some currently planned shaped pulses. These shaped pulses generally deliver about one-half the total laser energy over many nanoseconds with a high-intensity (10^{15}–10^{16} W/cm^2) peak delivering the remaining energy in less than 1 nsec. The low-density blowoff from such a temporally shaped pulse is likely to have a long scale length ideal for Brillouin backscatter of the high-intensity peak such as found in our experiment. Because the density of the backscatter region appears to be low ($n \lesssim 0.1n_c$), the ponderomotive force due to the final high-intensity laser peak is not likely to steepen this gradient. Indeed, the presence of stimulated scatter in longer-duration single-pulse experiments is suggested by the fact that backscatter from 250-psec is greater than for 100-psec pulses for irradiances in the mid-10^{15} W/cm^2 range.[5] Stimulated backscatter has also been observed in lower-irradiance 900-psec pulse experiments both with and without a prepulse.[4] It is obvious that experiments with the actual pulse shapes intended for laser-fusion designs are needed to determine how severe a problem Brillouin backscatter will actually be. The larger surface area irradiations expected in these designs could tend to increase the backscatter over that observed here.

It is a pleasure to acknowledge the laser expertise of J. M. McMahon which made these experiments possible and to thank R. W. Whitlock for aid during these experiments.

[1]J. L. Nuckolls, L. Wood, A. Thiessen, and G. Zimmerman, Nature (London) 239, 139 (1972).

[2]The term backscatter in this Letter refers only to the light scattered back into the solid angle of the focusing lens.

[3]S. E. Bodner and J. L. Eddleman, Lawrence Livermore Laboratory Report No.73378, 1971 (unpublished); C. S. Liu, M. N. Rosenbluth, and R. B. White, Phys. Fluids 17, 1211 (1974); D. W. Forslund, J. M. Kindel, and E. L. Lindman, Phys. Fluids 18, 1017 (1975); W. L. Kruer, E. J. Valeo, and K. G. Estabrook, Phys. Rev. Lett. 35, 1076 (1975); work by D. W. Phillion, W. L. Kruer, and V. C. Rupert (to be published) was brought to our attention since submittal of this Letter.

[4]B. H. Ripin, J. M. McMahon, E. A.McLean, W. M. Manheimer, and J. A. Stamper, Phys. Rev. Lett. 33, 634 (1974); L. M. Goldman, J. Soures, and M. J. Lubin, Phys. Rev. Lett. 31, 1184 (1973).

[5]B.H. Ripin, NRL Memo Report No. 3315, 1976 (unpublished).

[6]J. A. Stamper, Appl. Opt. 51, 2020 (1976).

[7]A much smaller effect upon backward reflection for prepulses with $\eta \gtrsim 10^{-4}$ ($4\% > R > 1\%$) was noted previous-

ly by A. A. Gorokhov, V. D. Dyatlov, V. B. Ivanov, R. N. Medvedev, and A. D. Starikov, Pis'ma Zh. Eksp. Teor. Fiz. 21, 62 (1975) [JETP Lett. 21, 28 (1975)]. See also Ref. 4.

[8]A 20% increase in scattered laser light for single-pulse irradiation has been observed when the target is moved out of the focal region of the lens although no irradiance dependence was noted between 5×10^{14} and 10^{16} W/cm^2. B. H. Ripin, in *Proceedings of the 1977 IEEE Conference on Plasma Science* (IEEE, New York, 1977), p. 66, and to be published. See also C. G. VanKessel *et al.*, Max Planck Institute Report No. IF IV/94, 1976 (unpublished).

[9]B. H. Ripin, Appl. Phys. Lett. 30, 134 (1977).

[10]The possiblity that the plasma blowoff may not be strictly one dimensional for grazing incidence is suggested by interferograms at normal incidence such as Fig. 3(c).

Electron Heating by Neutral-Beam Injection in the Oak Ridge Tokamak

M. Murakami, R. C. Isler, J. F. Lyon, C. E. Bush, L. A. Berry, J. L. Dunlap, G. R. Dyer, P. H. Edmonds, P. W. King, and D. H. McNeill
Oak Ridge National Laboratory, Oak Ridge, Tennessee 37830
(Received 19 May 1977)

Substantial electron heating by energetic-neutral-beam injection has been observed in Oak Ridge tokamak (ORMAK) plasmas. Impurity radiation is enhanced by injection but only to the degree expected for Ohmically heated discharges with the same total power input to electrons, and the electron heat conduction loss is comparable with that in Ohmically heated plasmas. The scaling of average electron temperature with total power input to electrons is approximately the same with or without injection.

Injection of energetic neutral beams is the principal method proposed for heating tokamak plasmas to fusion temperatures. While large increases in ion temperature with injection have been observed in ORMAK,[1] TFR,[2] and other tokamaks,[3] little, if any, electron heating has been reported. For substantial electron temperature increases with injection, the injection power delivered to electrons ($P_{\mathrm{inj},e}$) must significantly exceed the sum of (1) a reduction of Ohmic-heating power (due to the temperature increase and a possible injection-induced current[4]), and (2) an increase in electron power losses during injection (in particular, impurity radiation loss). In previous experiments[1,2] this requirement was not well satisfied, and the expected temperature increases have been within experimental uncertainties.

Here we report for the first time a substantial rise in the electron temperature with injection.[5] In comparison with our earlier work,[1] the heating was enhanced by higher available co-injection power (beam current parallel to discharge current) and by operation at lower impurity levels (lower effective ionic charge, Z_{eff}. In this Letter, we document observations of electron heating by injection and then present results that show an equivalence of Ohmic heating and injection powers in determining the scalings of electron temperature and power loss.

We first discuss in some detail the evolution of a plasma in which the injection heating is maximized by operation with injection power greater than the Ohmic-heating power. Figure 1 illustrates the behaviors of several parameters for this discharge. The discharge is sustained for 130 msec at a flat-top current of 70 kA with a toroidal field of 15 kG, giving a safety factor of 7 at the limiter radius of 23 cm. At 20 msec after breakdown, additional hydrogen gas is admitted to maintain the line-average electron density, $\bar{n}_e$, at $\approx 1.7\times10^{13}$ cm^{-3}. Injection to 340 kW

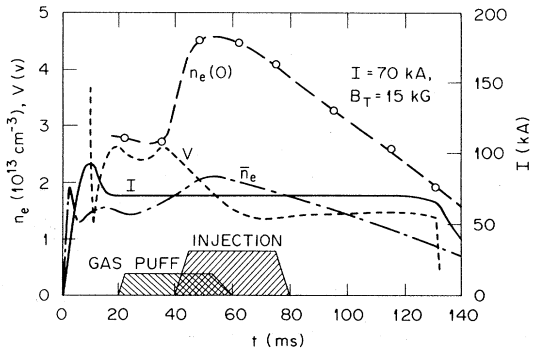

FIG. 1. Time histories of discharge parameters; plasma current (I), loop voltage (V), line-average electron density ($\bar{n}_e$), central electron density [$n_e(0)$], and timings of gas puffing and neutral-beam injection. The parameters shown here are those averaged over 42 reproducible discharges with 340-kW injection power.